Supplement of

Regional variability in black carbon and carbon monoxide ratio from long-term observations over East Asia: Assessment of representativeness for BC and CO emission inventories

Yongjoo Choi et al.

Correspondence to: Yongjoo Choi (choingjoo@jamstec.go.jp)

S1 Seasonal variation in dominant emission regions

Figure S2 shows the seasonal variation in data frequency and total mean fraction of dominant emission regions when APT was zero (without precipitation). Depending on the geographical characteristics, there is a distinct pattern of dominant emission regions. We decided that the valid dominant emission regions were only considered when the fraction of frequency was higher than 5% to ensure an adequate statistical analysis. As a result, Baengnyeong was suitable for monitoring the Chinese regions (East, North, and Northeast; 14–25%) and Korea (South and North; 8.1% and 16%, respectively), whereas Gosan was mainly influenced by the Chinese regions (11–20%) and South Korea (37%), along with a decreasing fraction of North Korea (4.2%). The Fukuoka and Noto sites were also good representatives for emission from Japan (51% and 58%, respectively); however, Fukuoka was good for East and North China (12% and 9.3%) and South Korea (20%), and Noto was good for Northeast China (22%) and South Korea (7.1%).

S2 Dry deposition effects

The basic assumption for this analysis is that the BC concentration does not show a significant decrease due to dry deposition during transport from the main source region. Similar to Kanaya et al. (2016), we investigated the effect of dry deposition on BC particles from the main source region to the receptor sites. Figure S3 is an example of a scatter plot between the ΔBC/ΔCO ratio and traveling time at the Noto site, with the mean value of each five-hour bin less than 72 hours. The slope of an exponential best fit line is very low as $1.32 \pm 1.88 \times 10^{-3}$ hour^{-1} (mean ± 95% confidence interval) which is correspondence to 0.02 cm s^{-1} for mean and 0.06 cm s^{-1} for upper 95% confidence interval of dry deposition velocities when mean mixing height was 646 m calculated from HYSPLIT model. Not only Noto site, but other three sites also showed the low dry deposition velocity in a range between 0.01 and 0.03 cm s^{-1}, suggesting the assumption is valid.

S3 The variation in the ΔBC/ΔCO ratio depends on the residence time

Since the ΔBC/ΔCO ratio could be influenced according to the residence time over the emission source regions, it should be investigated whether the variation in the ΔBC/ΔCO ratio depends on the residence time in the same dominant emission regions. Figure S4 shows the

mean ratio with standard deviation (vertical solid lines), divided by 20% intervals of the residence time fraction (total 73 hours) of the dominant emission region, along with a bar plot, which indicates the number of data for each bin. The open square symbols with a vertical dashed line indicate that the number of data was less than five (the 25th percentile of the number of data in each bin). We found that ΔBC/ΔCO did not vary significantly over the fraction of residence time when the number of data (N) was higher than five. The difference between each fraction in the same dominant emission region was statistically insignificant ($p > 0.05$), except for 'South Korea' in Fukuoka and 'Others' in Noto, when Welch's t-test and the analysis of variance (ANOVA) were applied to two and more than two groups, respectively. This result indicated that the variation in the ΔBC/ΔCO ratio according to the fraction (residence time) could be negligible when N exceeds five for the fraction of residence time. Hereafter, we used the data that satisfied the threshold ($N > 5$) of each bin for comparison with the REAS emission inventory. To verify whether these results were caused by the influence of other emission regions, the dominant emission region was constrained by considering only direct influence without passing through other emission regions. Although the constrained ΔBC/ΔCO ratios were only available for Korea and Japan, the mean ratios did not show a significant difference from the original ratio, implying that the effect of other emission regions was not significant.

S4 Footprint for Northeast China

Although the backward trajectory for Gosan passed a similar region as that for Baengnyeong (Figure S5) and the difference in the ΔBC/ΔCO ratio due to residence time is negligible, it is hard to exclude the possibility of mixing with emissions from South Korea from the beginning. The high ΔBC/ΔCO in the low residence time fraction for Northeast China in Gosan also supported the possibility of influence from South Korea (Figure S4).

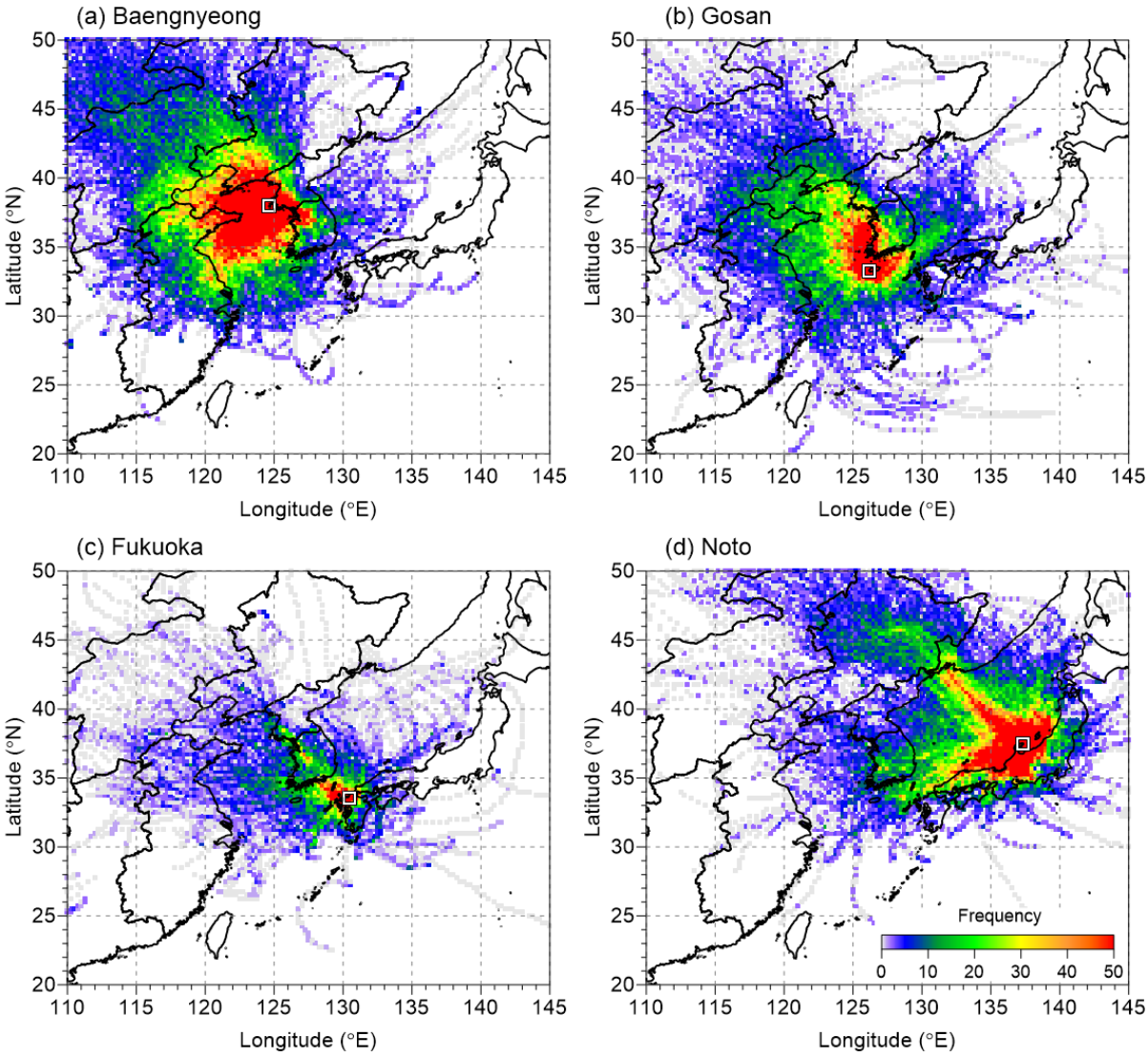

Figure S1. Footprint of the total number of backward trajectory endpoints for a 0.5°×0.5° grid cell depends on the measurement sites.

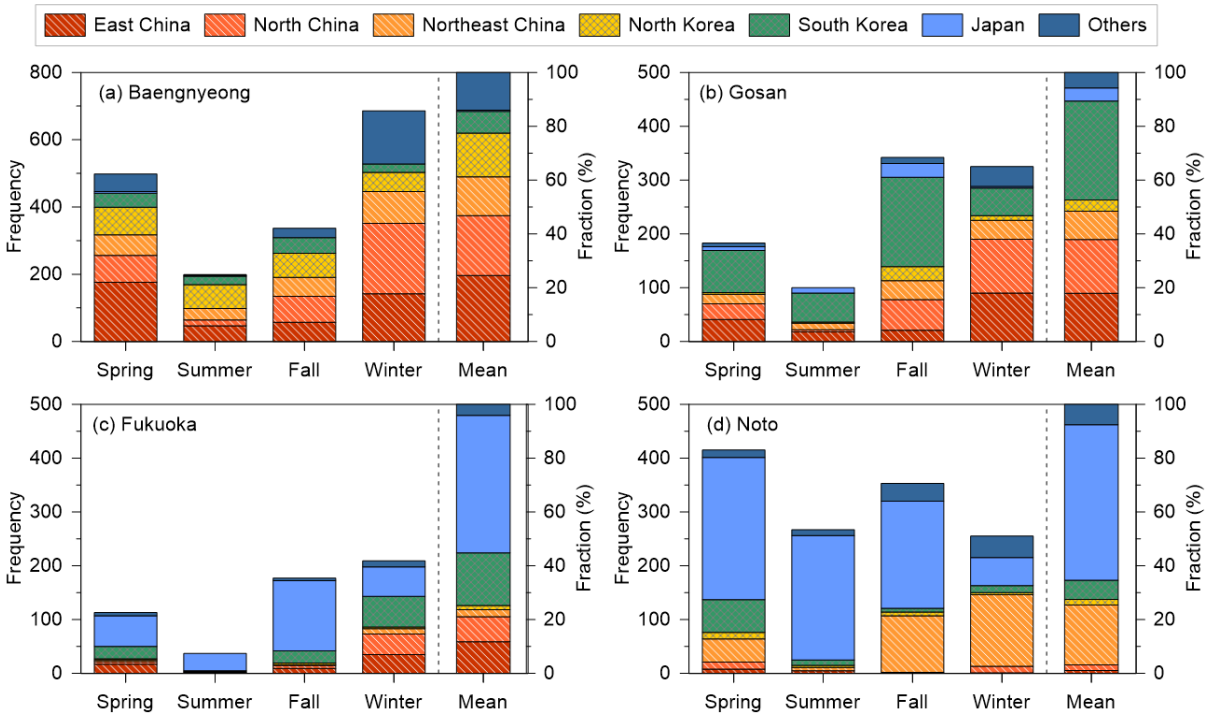

Figure S2. Seasonal variation in frequency (left side of dashed lines) and fraction (right side of dashed lines) for backward trajectory passed areas (dominant emission regions) in (a) Baengnyeong, (b) Gosan, (c) Fukuoka and (d) Noto.

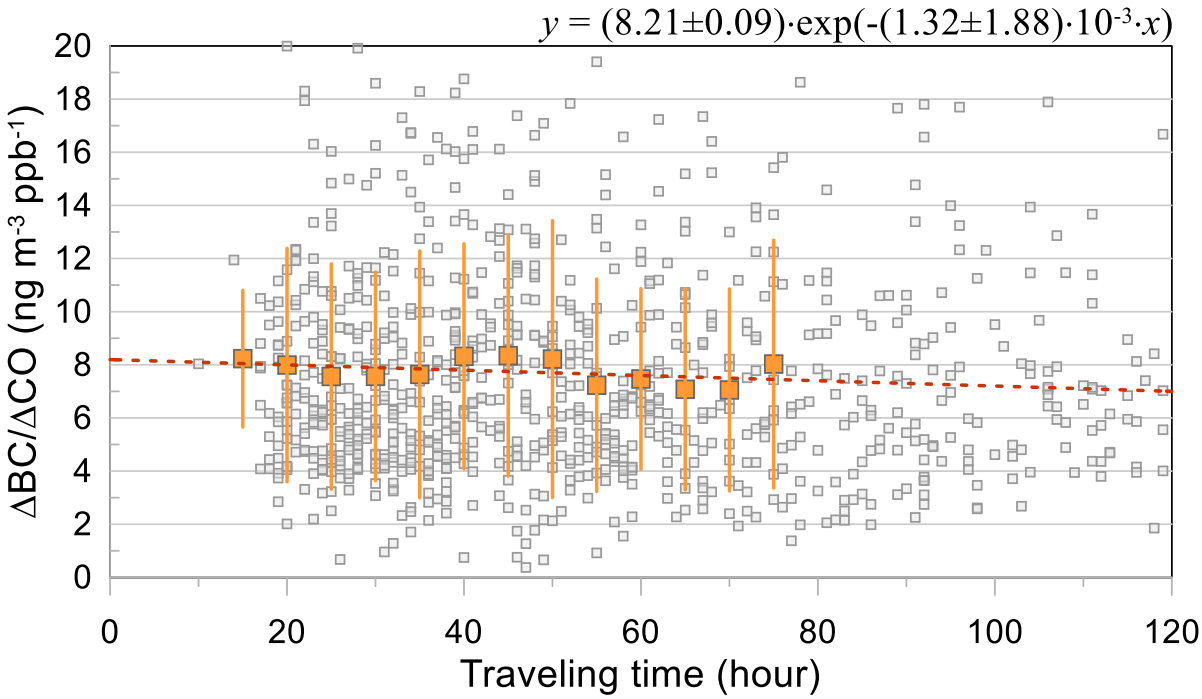

Figure S3. Scatter plot between ΔBC/ΔCO ratio and traveling time in Noto when APT was zero. The gray squares indicate every observed data point, and orange squares with vertical lines represent the mean and standard deviation of five hour bins less than 72 hours. The dashed line indicates the best fit line.

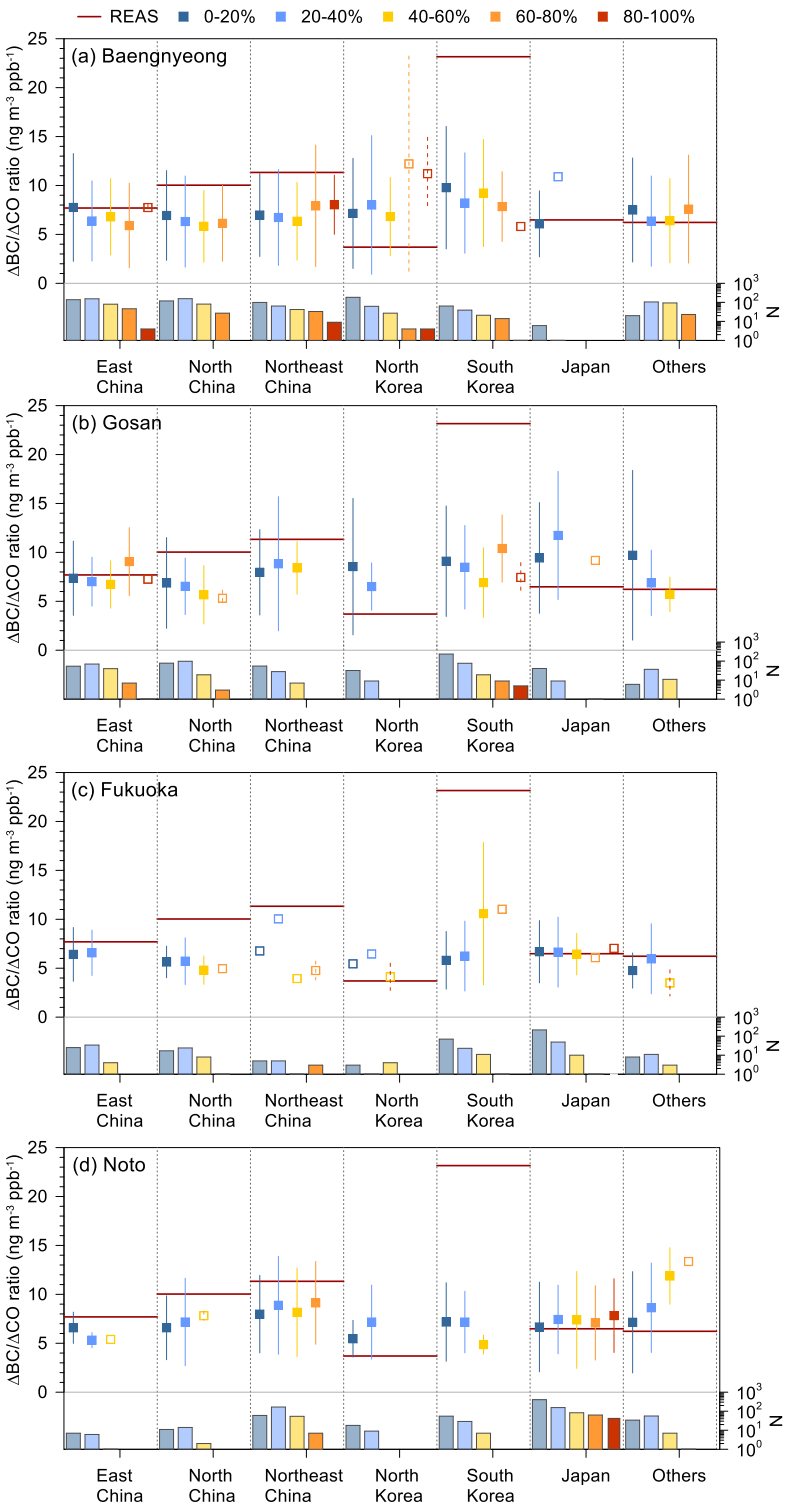

Figure S4. The measured ΔBC/ΔCO ratio in four measurement sites depends on the residence time fraction of the dominant emission regions. The color of the symbols with solid lines and the open symbols with dashed lines indicates the mean and standard deviation of each bin for the number of data (N) > 5 and $N \leq 5$, respectively. The bar graphs on the bottom indicate the number of data in each bin and the dominant region. The horizontal red lines depict BC/CO ration from REAS emission inventory.

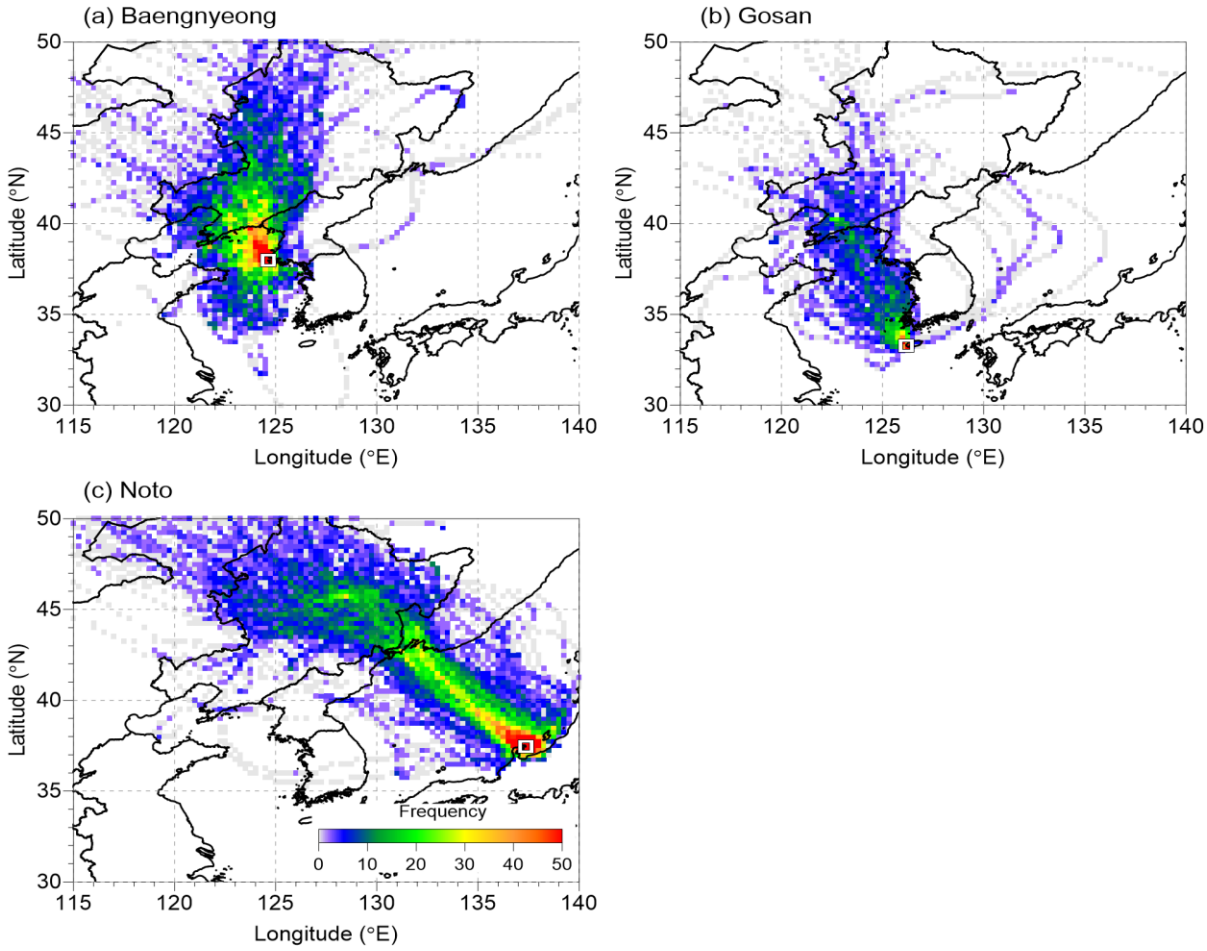

Figure S5. Same as Figure S1 except for the backward trajectory from Northeast China.

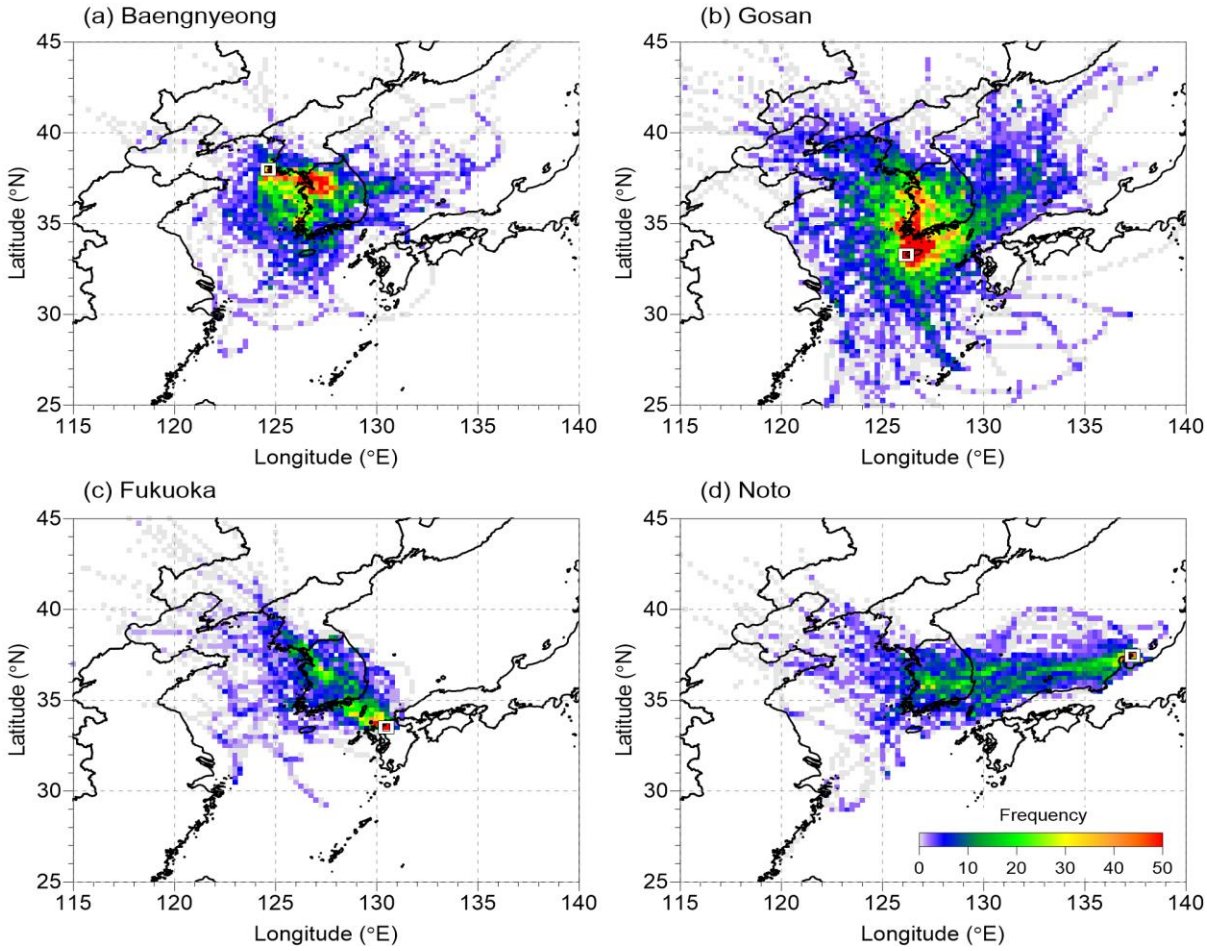

Figure S6. Same as Figure S1 except for the backward trajectory from South Korea.

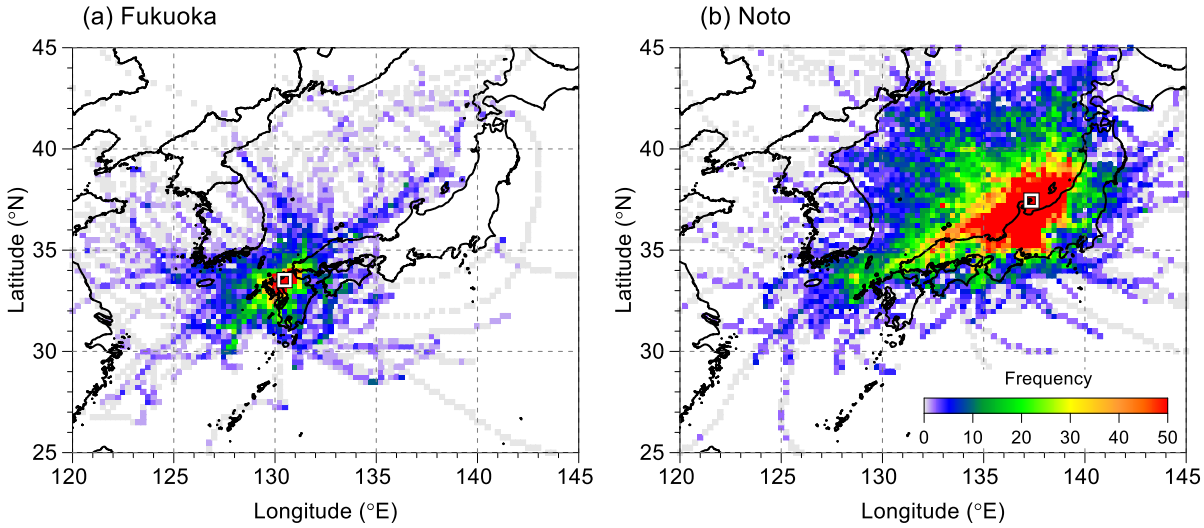

Figure S7. Same as Figure S1 except for the backward trajectory from Japan.